IJST, Transactions of Civil Engineering, Vol. 39, No. C1, pp 125-141
Printed in The Islamic Republic of Iran, 2015
© Shiraz University

A COMPARATIVE NUMERICAL STUDY OF A GEOSYNTHETIC-REINFORCED SOIL WALL USING THREE DIFFERENT CONSTITUTIVE SOIL MODELS*

E. SEYEDI HOSSEININIA**
Dept. of Civil Engineering, Faculty of Engineering, Ferdowsi University of Mashhad, Mashhad, I. R. of Iran
Email: eseyedi@um.ac.ir

Abstract– In this paper, three different soil constitutive models for granular soils were implemented in the numerical simulation of a full-scale reinforced soil segmental wall in order to predict the wall response during construction. The soil constitutive models in the order of complexity are: linear elastic-perfectly plastic Mohr-Coulomb, Duncan-Chang hyperbolic, and a nonlinear elastic-plastic hardening model. The latter, which can be regarded as a modified version of the Mohr-Coulomb model, captures the nonlinear stress-dependent soil response. The nonlinear model can consider soil dilative behavior. In this regard, it keeps the simplicity in the formulation together with the accuracy in the prediction of soil response. By comparing the results, in general, there is good and acceptable accordance between numerical simulations and field measurements. It is seen that using a simple soil model can acceptably predict the performance of reinforced walls. However, the disadvantage relates to poorness in the prediction of wall facing displacement, which is sensitive to proper consideration of deformation parameters in a soil model. The accuracy of the prediction can be augmented by adopting reasonable functions for elastic (stiffness) and plastic (dilatancy) parameters with respect to the stress condition within the soil backfill.

Keywords– Soil constitutive models, reinforced soil wall, response prediction, numerical analysis, geosynthetic reinforcements, soil dilatancy

1. INTRODUCTION

Numerical methods such as finite element or finite difference methods are now widely used for analyzing the mechanical behavior of Geosynthetic Reinforced Soil (GRS) walls [1, 2-5]. Since design methods used for these structures are based on analytical methods [6-8], they do not account for deformation states anymore. Many studies indicate that these methods are extensively conservative and predicted loads and deformations in soil and reinforcements do not correlate with measured values [9,4,10,11]. Numerical methods facilitate better understanding of the performance of these soil structures and thus, they can be considered as new steps in the optimization of design methods [12, 13-15].

One of the challenges in the numerical methods is the choice of soil constitutive model. There should be a balance between the simplicity, applicability, and the prediction accuracy of the constitutive model. Advanced soil models can predict more accurately the stress-strain relationship than simpler soil models, but they require a large number of parameters or the parameters cannot be easily determined from routine laboratory testing. In addition, the analysis might be time-consuming and expensive, and thus impractical.

To verify of the results of numerical analyses with full-scaled reinforced soil walls [16,17-20], the model behavior of backfill soil is of great Importance. In the case of extensible reinforcements, Hatami and Bathurst [17] and Huang et al. [21] showed that the implication of Mohr-Coulomb model gave good agreement with the measured wall displacements and boundary toe forces, but resulted in a poorer

*Received by the editors February 9, 2013; Accepted February 5, 2014.
**Corresponding author

prediction of strain levels in reinforcement layers. Although working with such a simple model seems to be comfortable and practical to the engineers, the problem arises in the challenge of selecting suitable soil parameters. Generally, such a simple model is best suited for the analysis of reinforced soil walls at the state of incipient failure rather than for service conditions. The other simple soil model used widely in the numerical simulation of reinforced soil walls, is Duncan-Chang model, since it considers a nonlinear stress-strain relationship as well as variable soil stiffness in the formulation [18, 19, 22, 23, 12]. However, the disadvantage of the model is the inability to consider a correct prediction of dilative behavior. Karpurapu and Bathurst [24] showed that the soil dilation has a significant effect on the prediction accuracy of the performance features of reinforced soil walls. They could consider the soil dilation by using a numerical technique within the finite element formulation in order to use the hyperbolic model in conjunction with the classical plasticity theory. The technique concerns the update of stiffness matrix according to the stress state. It is noted, however, that this technique is not straight-forward and cannot be implemented easily in any numerical code. An alternative solution is to use advanced soil models, which can take into account the contractive/dilative behavior of the soil.

Sophisticated analyses by using advanced constitutive soil models have been recently implemented in the numerical analysis of reinforced soil walls. Among them, Desai and El-Hoseiny [25] used an advanced soil model with 12 parameters, based on the disturbed state concept (DSC) in a finite element code for the prediction of field performance of a GRS wall behavior during construction. Ling et al. [26] used a generalized plasticity model in static and dynamic analyses of reinforced soil walls. The model in total requires 15 parameters, however, 11 of them can be obtained from static tests. Ling and Liu [27] used both of these models in simulating the behavior of a reinforced soil segmental wall and they found that both models gave almost similar results for different features of the wall behavior. In another attempt, Huang et al. [21] compared the results of numerical simulation of reinforced soil walls obtained from three types of soil constitutive models including Mohr-Coulomb, Duncan-Chang and Lade models. The latter is an advanced soil model with the capability of considering intermediate principal stress and good prediction of soil undrained behavior [28]. The parameters of the Lade model can be obtained from conventional (like triaxial compression) tests. However, its disadvantage, similar to the DSC and generalized plasticity models, is a number of parameters in the formulation (twelve parameters) as well as the lack of obvious physical meaning of the parameters. The comparison indicated that the advanced soil model did not necessarily give a better result than simpler models. They concluded that the modified Duncan-Chang model is a good compromise between prediction accuracy and availability of parameters from conventional triaxial compression test. Abdelouhab et al. [29] have reached the same conclusion by comparing the simple Mohr-Coulomb and Duncan-Chang models with an advanced soil model in an extensive parametric numerical study of reinforced soil walls.

In order to support the simplicity together with the accuracy in the analysis of reinforced soil media, Seyedi Hosseininia and Farzaneh [30] introduced a relatively simple soil constitutive model in the framework of bounding surface plasticity. The soil model is formulated for non-cohesive granular soils. It can simulate the non-linearity of stress-strain relationship as well as dilative/contractive behavior of the soil. They used the model combined with two-phase concept [31], which is regarded as a new class of homogenization methods. The algorithm has been aimed to be applied to the analysis of reinforced soil structures under operational conditions focusing on geosynthetics-reinforced soil walls. The soil model has been formulated in such a way that the least number of parameters be required and the values can be determined easily from conventional laboratory testing as well. The applicability of the soil model has been evaluated in the domain of homogenization of reinforced soil medium as a two-phase system. In this paper, the proposed soil constitutive model will be used in a discrete modeling of reinforced soil system and the behavior of a full-scale well documented reinforced soil wall is investigated numerically. Besides, a comparative study with the Mohr-Coulomb and Duncan-Chang models will be done in order to show the efficiency of the proposed soil model.

2. A BRIEF REVIEW OF SOIL CONSTITUTIVE MODELS

In this study, the implication of three types of soil constitutive models in the numerical simulation of reinforced soil walls is examined. These models in order of increasing complexity are as follows: 1) linear elastic-perfectly plastic Mohr-Coulomb; 2) Duncan-Chang hyperbolic; and 3) a nonlinear elastic-plastic hardening model based on Mohr-Coulomb failure criterion. In this paper, the latter is named nonlinear Mohr-Coulomb model. In what follows, a summary of each model characteristics is described and the laboratorial behavior of a silty sand is simulated.

a) Mohr-Coulomb model

This model has been defined in the classical framework of incremental plasticity. The behavior decomposes into two parts as elastic and plastic. The elastic part is linear and obeys the generalized Hooke's law with constant Young modulus (E) and constant Poisson's ratio (ν). Other equivalent moduli named shear modulus (G) and bulk modulus (K) are often used too. The plastic state of the behavior is defined by the Mohr-Coulomb yield criterion with the parameters friction angle (ϕ) and cohesion (c), which is also known as yield surface in the space of major and minor principal stress components. The model is perfectly plastic, which indicates that the yield surface is fixed in the stress space and the soil has a constant rate of plastic deformation along with further loading. In order to prevent an excessive prediction of soil dilation, a plastic potential function was defined by a parameter called dilation angle (ψ) in place of ϕ in the yield function [32, 33]. Accordingly, the linear elastic- perfectly plastic Mohr-Coulomb model consists of a total of five parameters describing shear strength (ϕ, c) and deformation (E, ν, ψ) properties.

The Mohr-Coulomb model is very attractive in geotechnical problem analyses since the formulation and thus, the implication of the model in numerical codes is simple. In addition, the parameters generally have physical meaning to the geotechnical engineers. However, the major disadvantage of the model is the challenge in determining the values of the parameters from routine laboratory testing. In the literature there have been some attempts to define the parameters from the curves obtained in laboratory [34], but the problem still exists, keeping in mind that the soil behavior is highly dependant upon different initial states such as confining pressure. Holtz and Lee [23] demonstrated that considering the effect of confining pressure in the soil behavior is an important issue in accurately predicting the wall face deformation. Hence, a set of tests with different confining pressures should be considered as a database in order to find the appropriate values of backfill soil parameters.

b) Duncan-Chang model

The Duncan-Chang model is formulated based on triaxial compression test results [35, 36]. The formulation considers only the elastic behavior of the soil with a nonlinear hyperbolic function. The model formulation is based on the generalized Hooke's law and hence, Young modulus (E) and Poisson's ratio (ν) are required. ν can be supposed constant, but the slope of the stress-strain relationship is variable and the elastic tangent modulus (E_t) is expressed as a stress-dependent form:

$$E_t = \left[1 - R_f \frac{\sigma_1 - \sigma_3}{(\sigma_1 - \sigma_3)_f}\right]^2 K p_a \left(\frac{\sigma_3}{p_a}\right)^n \tag{1}$$

where σ_1, σ_3 are the major and minor principal stresses, respectively. p_a is the atmospheric pressure (=101 kPa). R_f, K, and n are model parameters representing the failure ratio, elastic modulus number, and elastic modulus exponent, respectively. The term $(\sigma_1 - \sigma_3)_f$ stands for the deviatoric stress at failure obtained from laboratory test results and is equal to:

$$(\sigma_1 - \sigma_3)_f = \frac{2c\cos\phi + 2\sigma_3 \sin\phi}{1 - \sin\phi} \tag{2}$$

The disadvantages of the model are: a) the model can only predict the initial hardening behavior of the soil model till the peak shear strength and not the post-peak softening behavior; b) the model cannot simulate the stress-strain path in plane strain loading condition; c) the model cannot take into account the dilative behavior, i.e., the soil dilatancy.

c) Nonlinear Mohr-Coulomb model

The third model evaluated in the present study is a relatively simple elastic-plastic soil model introduced by Seyedi Hosseininia and Farzaneh [30]. The model is dedicated to the problems in which 1) soil experiences monotonic stress paths and cyclic loading is out of scope of the model; 2) high variations of stress level and/or density in the soil do not exist; 3) the post peak (softening) behavior and large level of deformation in the soil is not expected. The formulation of the model, which is presented on the effective stress basis, has been introduced in such a way that the least number of parameters be required. In addition, the parameters have physical meaning to the engineers and all of the parameters can be captured from both routine (e.g., triaxial) and non-routine (e.g., plane strain) laboratory testing. Finally, the framework of the constitutive model is improvable for future extensions in order to consider other aspects of the soil behavior such as density, critical state, anisotropy, cyclic loading, etc. Note that the model formulation has been presented for non-cohesive soils. The principles of the model and the constituents have been described in detail by Seyedi Hosseininia and Farzaneh [30] and a brief scheme of the model is described below.

The global concept of the model is similar to the Mohr-Coulomb model mentioned above and the major modifications have been applied to the incremental stress-strain relationships. In the elastic part, the generalized Hooke's law is taken into account in terms of a constant Poisson's ratio (ν) and a variable shear modulus (G) as follows:

$$G = G_0 \left(\frac{p}{p_a} \right)^n \tag{3}$$

p is mean pressure ($= (\sigma_1 + \sigma_2 + \sigma_3)/3$) in which, σ_2 is the intermediate principal stress. G_0 is the initial shear modulus of the soil at the atmospheric pressure and n is the exponent of the relationship. These two parameters can be easily obtained from a series of laboratory testing (at least three tests) with the same density (or void ratio equivalently), but with different confining pressure.

For the plastic part of the strain increment, the formulation has been introduced in the framework of bounding surface plasticity [37-40]. Based on this framework, a yield surface always remains inside a limiting bound technically called bounding surface. Both the yield and bounding surfaces have a wedge form in the principal stress space similar to the Mohr-Coulomb yield surface. Similar to the Mohr-Coulomb criterion, the intermediate principal stress plays no role in the plastic part (magnitude and direction of plastic strain increment) of the model either. The initial size of the yield surface is zero. Form the onset of loading, however, the yield surface expands isotropically so that it coincides with the bounding surface. The size of the yield function at each stress state is defined by the mobilized friction angle of the soil (ϕ_{mob}) defined as follows:

$$\phi_{mob} = \sin^{-1}\left(\frac{\sigma_1 - \sigma_3}{\sigma_1 + \sigma_3} \right) \tag{4}$$

The upper bound size of the bounding surface is equal to the peak friction angle of the soil (ϕ_{peak}).

According to the bounding surface plasticity theory [41], the distance between the surfaces is defined by the plastic modulus (K_p), whose form in the proposed model has been defined:

$$K_p = h_0 G\left(\frac{\sin\phi_{peak} - \sin\phi_{mob}}{\sin\phi_{mob}}\right) \tag{5}$$

where h_0 is a positive model parameter. In the bounding surface formulation, the inverse value of the plastic modulus controls the volume change response.

In the formulation, the plastic deformation of the soil is taken into consideration from the beginning of shear loading. In theory of plasticity for geomaterials, the plastic part of deformation (dilation or contraction) is captured by defining a dilatancy function (D), which explains the relationship between volumetric and deviatoric plastic strain increments. The D function in the proposed model has the following form:

$$D = D_0(\sin\phi_{mob} - \sin\phi_{PTL}) \tag{6}$$

D_0 is a model parameter that defines the tendency to dilate ($D > 0$) or contract ($D \le 0$). Parameter ϕ_{PTL} is defined as the mobilized friction angle at which, the soil behavior is transformed from being contractive to dilative. If the soil is loose, it tends to contract and ϕ_{PTL} has a value close or equal to ϕ_{peak}. It is noted that the value of the dilatancy function in a perfectly-plastic model keeps constant. Knowing that the dilation angle (ψ) in the Mohr-Coulomb model is defined as the ratio of volumetric plastic strain increment to the shear plastic strain increment, we have: $D = \sin\psi$, where ψ was introduced before as the dilation angle.

Totally, the proposed model has seven parameters including elastic (G_0, n, ν), shear strength (ϕ_{peak}), dilatancy (ϕ_{PTL}, D_0), and hardening (h_0) parameters. All the parameters can be determined from a minimum of three sets of tests with the same density and different stress levels. The procedure of the parameters derivation and calibration from a set of stress-strain curves is explained by Seyedi Hosseininia and Farzaneh [30].

d) Comparison of constitutive soil models

In this part, the laboratorial behavior of a soil is simulated by virtue of the three soil models discussed above. The soil is silty sand ($D_{50} = 0.42\,mm, \gamma = 16kN/m^3, C_u = 4.6$), which was used as the backfill material in the construction of a full scale 6-meter reinforced soil wall that is described in the next section. The study has been performed by conventional drained triaxial compression tests under confining pressures of 25, 50, and 100 kPa.

The parameters of all models are classified into four groups of shear strength, dilatancy, elastic, and hardening parameters and the corresponding values are presented in Table 1. Since the Duncan-Chang model only predicts the contractive trend in the soil deformational behavior, the Poisson's ratio for this model is chosen a little higher in order to have a better prediction of the soil behavior. The laboratorial together with the simulated behaviors of the samples are depicted in Fig. 1 in terms of deviatoric stress and volumetric strain versus axial strain. Fig. 1a shows the deviatoric stress and volumetric strain variations in terms of axial strain by using the Mohr-Coulomb model. Similarly, the Duncan-Chang model is used in order to predict the samples behaviors. According to Fig. 1b and in comparison with Fig. 1a, it is seen that the Duncan-Chang model can well reflect the nonlinearity of deviatoric stress as well as the increase in the initial elastic modulus with confining pressure. However, the dilative behavior of the soil is not predictable by the model. By using the nonlinear Mohr-Coulomb model, it can predict well the nonlinearity existed in the curves of deviatoric stress and volumetric strain of the samples, as shown in Fig. 1c. As explained before, the post peak (softening) behavior at large strain levels is out of scope of the model.

Table 1. Soil parameters used in the simulation of samples behavior

Shear Strength		Dilatancy		Elasticity			Hardening
Mohr-Coulomb Model							
ϕ (degree)		ψ (degree)		E (MPa)		ν (-)	-
39		6		25		0.2	-
Duncan-Chang Model							
ϕ (degree)	R_f (-)	-		K (-)	n (-)	ν (-)	-
39	0.81	-		263	0.5	0.25	-
Nonlinear Mohr-Coulomb Model							
ϕ_{peak} (degree)		ϕ_{PTL} (degree)	D_0 (-)	G_0 (MPa)	n (-)	ν (-)	h_0 (-)
39		33	1.6	11.1	0.5	0.2	0.37
γ (unit weight, kN/m^3)				16			

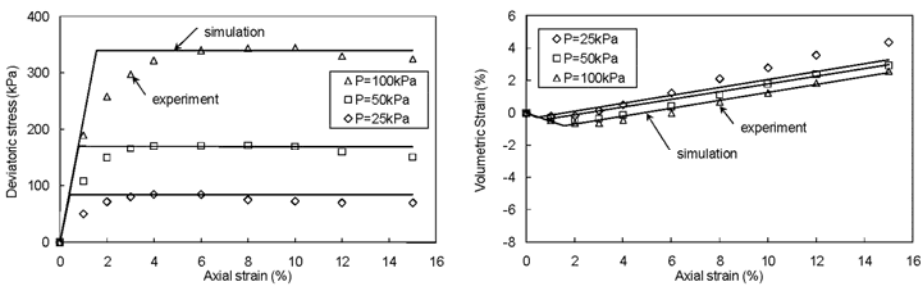

(a) Mohr-Coulomb Model

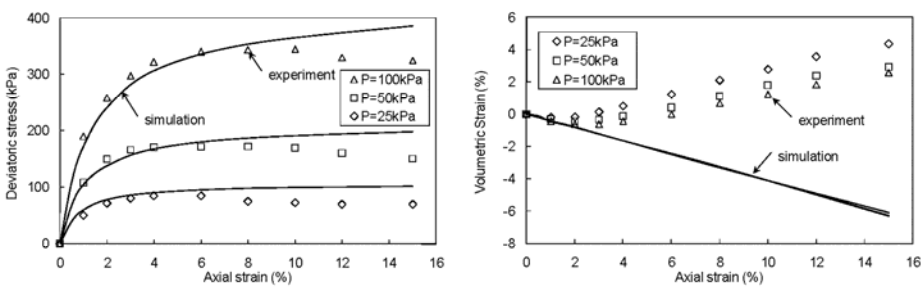

(b) Duncan-Chang Model

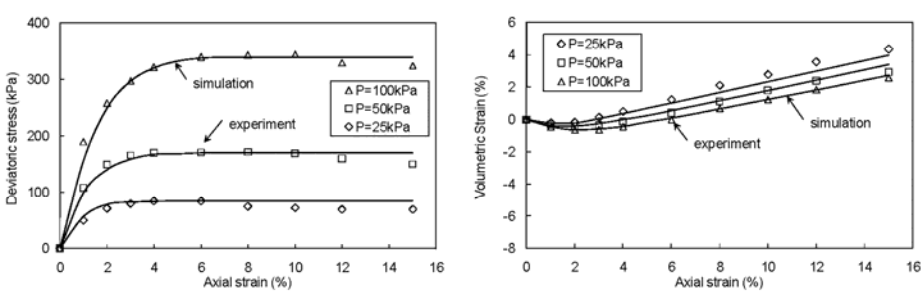

(c) Non-linear Mohr-Coulomb Model

Fig. 1. Soil behavior in terms of deviatoric stress and volumetric strain versus axial strain obtined from laboratorial triaxial compression testing and simulation by different soil models (experimental data from Ling et al. [26])

3. NUMERICAL MODELING OF A REINFORCED SOIL WALL

A reinforced soil wall that has a block-type facing is nominated here in order to investigate the applicability and comparison of the soil constitutive models cited in this work. The wall was constructed and instrumented by the Public Works Research Institute (PWRI) in Tsukuba, Japan. This well documented case history was undertaken to monitor the construction behavior of the wall. Basic information of the PWRI wall has been reported by Tajiri et al. [42].

It must be noted that the wall has already been studied and evaluated numerically by adopting hyperbolic Duncan-Chang and generalized plasticity models for the backfill soil material [27]. In addition, a membrane analogy method has been presented to evaluate the deflection of fabric-reinforced earth walls [43]. In this method, the governing equations were solved by using finite difference method.

The present study is an extra investigation to explore the influence of different soil constitutive models on the prediction of wall performance features and to compare the results with measured response. The present work is distinguished from the previous numerical studies in three parts: 1) the numerical method used in this research is finite difference method, while the previous simulations were carried out by finite element method; 2) the Mohr-Coulomb and a simple nonlinear elastic-plastic soil model are implemented for the backfill soil, which were not used before. Although the Duncan-Chang model was already used, it is implemented again in the present study to compare the simulations; 3) a linear elastic model is dedicated to the reinforcement component, while advanced nonlinear constitutive models were applied in the previous numerical studies.

The same parameters obtained from conventional triaxial testing are used in the simulations. In order to avoid local numerical instabilities within the soil backfill in the numerical analyses, a small cohesion value (c = 0.2 kPa) is assumed when using Mohr-Coulomb and Duncan-Chang models and a small initial value for the mobilized friction angle ($\phi_{mob} = 5^{\circ}$) is considered when using the nonlinear Mohr-Coulomb model.

All simulations of the reinforced soil wall in the current study were carried out using the finite-difference-based code FLAC [44]. For the case of Mohr-Coulomb and Duncan-Chang models, The FLAC library models were used, while the nonlinear Mohr-Coulomb model was coded and implemented in FLAC using the programming language FISH (UDM option).

a) Wall description

The configuration of the wall and the numerical mesh used in the numerical analysis is depicted in Fig. 2a and 2b, respectively. The total wall height is 6 m. The backfill material was made of silty sand whose behavior was described and numerically simulated in the previous section. It is noted here that the parameters of soil models have been obtained from the confining pressure levels (25, 50, and 100kPa) in the triaxial tests that are consistent with the stress level generated through the total wall height.

The face of the wall was constructed by 12 concrete blocks, each 50 cm high and 35 cm wide, except for the top and bottom blocks that were 45 cm and 35 cm high, respectively. The blocks were back supported by geosynthetic layers bolted together by nuts and metal frame. The layers consisted of six primary (3.5 m long) and five secondary (1.0 m long) geogrids. The wall was constructed directly on a concrete floor inside a test pit.

The wall was well instrumented in order to trace its behavior during the construction. A total of 52 strain gauges were used to measure the elongation of both primary and secondary geogrid layers. The horizontal displacement of the wall facing was measured at 11 locations by using linear variable displacement transducers (LVDT). The lateral pressure acting against the back of the facing blocks (11 locations) together with the vertical pressure due to the backfill soil along the base (6 locations) were also measured during construction.

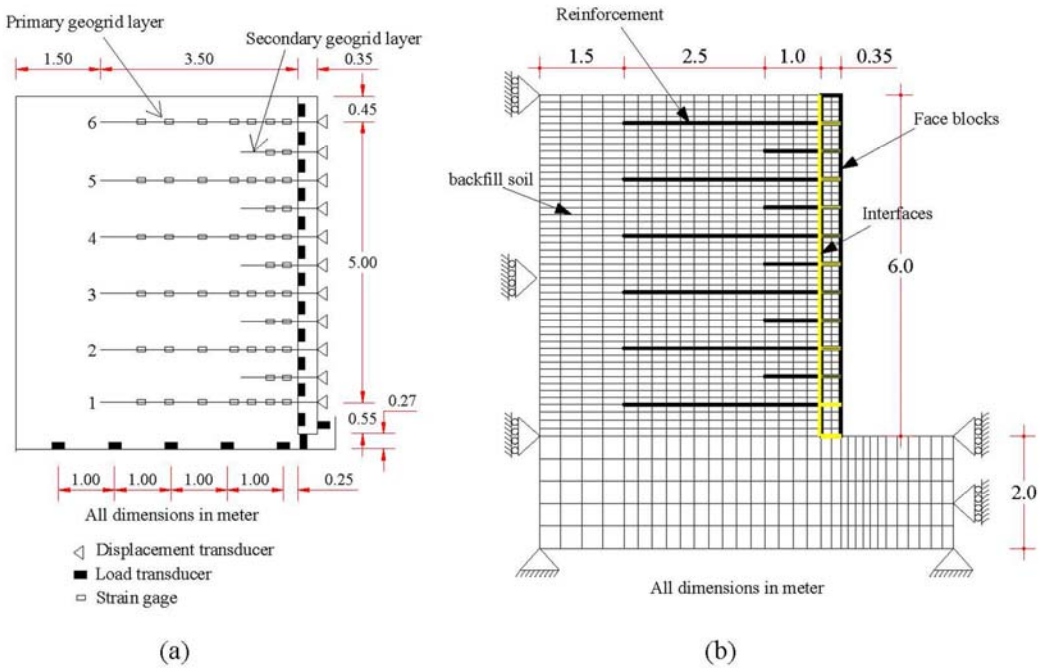

Fig. 2. Scheme of the PWRI wall: (a) geometry and instrumentation; (b) numerical model used in the analysis

b) Reinforcements

In the wall construction, a uniaxial geogrid, manufactured from extruded high-density polyethylene (HDPE) was used as the reinforcement layers. The load-strain curve of a uniaxial tensile test on the geogrid at a strain rate of 1% per minute is shown in Fig. 3. The axial tensile stress in the geogrid increases almost nonlinearly, especially as the axial strain increases. In the numerical analysis, however, it is assumed that the geogrid layer obeys linear elastic behavior by using a linear tensile element in the numerical analysis. This simplification is admissible since the instrumentation indicated that the maximum strain tolerated by the geogrids at the end of construction hardly reached 1%. Hence, for the reinforcement, a constant tensile stiffness (J) equal to 720 kN/m is chosen, which is fitted on the laboratory curve according to Fig. 3. In numerical simulation, the reinforcement layers are fixed to the back of the facing blocks with free rotation. For more detailed information, refer to Tajiri et al. [42].

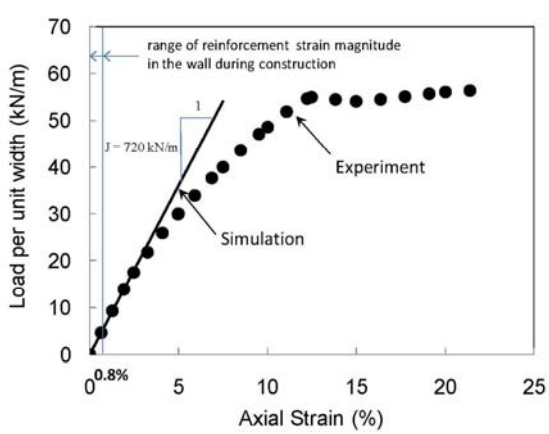

Fig. 3. Uniaxial load-strain response of HDPE geogrid and the behavior approximation adjusted for small range of strain. Note that the reinforcement experienced maximum strain magnitude of 0.8% during construction.

c) Blocks, foundation, and interfaces

Other material and interaction properties in the analysis are considered similar to those reported by Ling et al. [19] and they are explained here briefly. The facing blocks and the foundation of the wall, which were made of concrete, are assumed to be linear elastic. The values of the properties are: $E = 2.0GPa, \nu = 0.17, \gamma = 23kN/m^3$. The friction angle of the interfaces for the block-block and soil-block interactions are considered to be 19.6° and 16.5°, respectively, which were obtained from large scale direct shear tests. The normal (k_n) and tangential (k_t) stiffness of block-block and soil-block interface elements are taken as $k_n = 10^9 Pa/m, k_s = 10^8 Pa/m$, and $k_n = 10^8 Pa/m, k_s = 10^6 Pa/m$, respectively. No interface element is used between the geogrid layers and the backfill soil, because it is assumed that the geogrids are fully bonded to the soil. For more detailed information, refer to Tajiri et al. [42].

4. COMPARISON OF RESULTS

Results of the analyses are compared with the measured data obtained from the instrumentation.

a) Wall facing displacement

Figure 4 shows the calculated and measured facing displacements at the end of construction in five stages of H = 2, 3, 4, 5, and 6 m. This plot concerns the horizontal component of the facing displacement. The measured data is depicted by a dash line, while the contour of the deformed facing is marked with a solid line. In neither of the analyses does the wall deformation at the construction heights of 2 and 3 m match the measured data. None of the previous numerical analyses predicted the wall facing profile for these heights. This discrepancy would be because of unknown features, which are not considered in numerical modeling such as the effect of compaction of filling layers or reinforcement connection details. For the rest, based on the comparison of the results, it is determined that using all three types of soil constitutive models can suitably capture the global profile of facing deformation. However, the predictions have different levels of accuracy.

The analysis with the Mohr-Coulomb model underestimates the lateral displacement. The discrepancy increases more at around the middle of the height. The analysis using the Duncan-Chang model shows that the facing blocks are moved relative to each other more than that using Mohr-Coulomb model. This causes that the latter case globally over predicts the wall lateral displacement. By paying attention to the characteristics of these two models in simulating the soil behavior (Fig. 1a,b), such kind of difference in the response can be explained by the deformation behavior of the soil; first, the stiffness of the soil is underestimated and, second, the dilative behavior of the soil cannot be captured by the Duncan-Chang model. This issue will be discussed in the next section. Similar to the case of Mohr-Coulomb model, the calculated results using the Duncan-Chang model are close to the measurement at the top of the wall, but the discrepancy rises at lower parts of the wall height. It must be noted that the results of the present paper are consistent with that of Ling et al. [19] by using Duncan-Chang model. Finally, referring to the results obtained by the nonlinear Mohr-Coulomb model, it can be seen that the outline of the wall obtained from the simulation is favorably compatible with the measured trace of the facing. Unlike other soil models, this accordance exists along the whole of the wall height. It is reminded that the prominence of this model to the others is the ability to capture both the elastic stiffness variation and the dilative behavior of the soil.

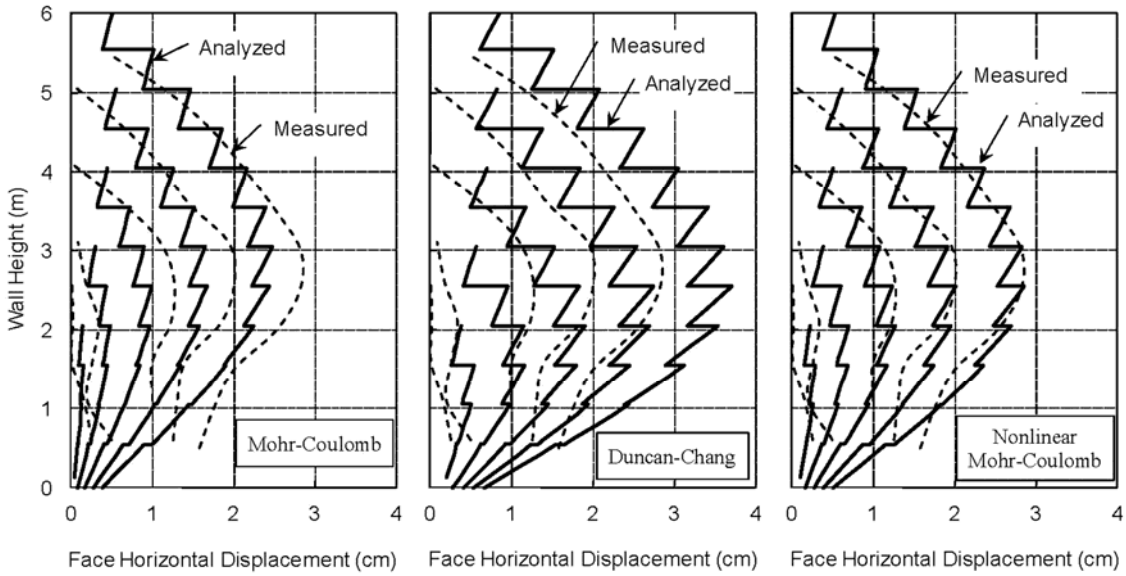

Fig. 4. Comparison of the horizontal displacement of the facing obtained from the measured and simulation results

b) Lateral pressure at the back of the facing

Figure 5 presents the distribution of the horizontal pressure at the back of the wall facing obtained from the measurement and numerical analyses. As shown, the results obtained from all analyses give a similar trend, whose values are almost coincident with each other. In addition, the distributions obtained from the analyses agree well with the measured data. It can be concluded that the soil model does not have an influence on the prediction accuracy of the distribution of lateral pressure at the back of the segmental blocks. The zigzag pattern shown in the lateral pressure distribution pertains to the stress concentration by the reinforcement layers, which have perfect contact with the adjacent soil layer.

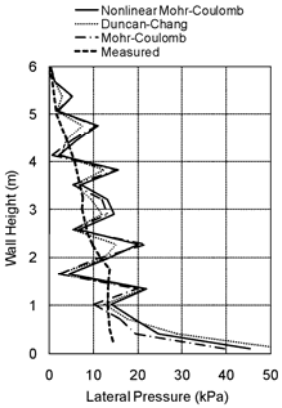

Fig. 5. Comparison of predictions of lateral stress at the back of the wall facing with measured data

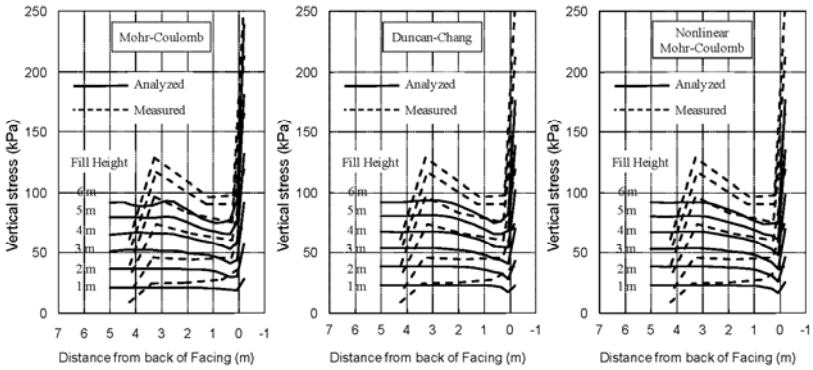

Fig. 6. Vertical stress distribution on the foundation of the wall obtained from instrumentation and numerical analyses

c) Vertical stress over the wall foundation

The distributions of vertical stress at the base of the backfill and at the bottom of facing blocks are depicted in Fig. 6 for different heights of the wall construction. Comparison of the calculated results from different soil models reveals that using all soil models in the numerical simulations gave similar

distribution of vertical stress. In other words, considering the nonlinearity in the stress-strain relationship and the deformation behavior (dilatancy or contraction) in the soil model does not influence the prediction of the vertical stress distribution over the foundation.

d) Reinforcement strains

The measured and simulated strain distribution of six primary geogrid layers contributed to the end of construction (H = 6 m) is depicted in Fig. 7. As a general observation, the predicted distribution of strains using all soil models is in good agreement with the measured results. According to Ling et al. [26], the discrepancy observed for the first and third primary layers at the front location could be attributed to the possible stress concentration because of uncommon connection (bolt and nut) of geogrid to blocks as well as creep in the geogrid that were not considered in the numerical modeling.

Comparison of the calculated results from the numerical analyses reveals that the predictions of reinforcement strains by the linear elastic-plastic Mohr-Coulomb and the nonlinear Mohr-Coulomb models are approximately coincident. However, using Duncan-Chang model in the analysis leads to larger values of strains, which recedes from the measured data. The dissimilarity between these two groups increases for the reinforcements situated at the lower parts of the wall. Referring to the soil models characteristics, it can be concluded that such difference in the predictions corresponds to the dilative behavior, because the Duncan-Chang model, unlike the other models, cannot take into account the soil dilatancy. This result is consistent with the comparative study performed by Ling and Lieu [27], where the reinforcement strains with the Duncan-Chang model were generally calculated higher than those with the generalized plasticity model.

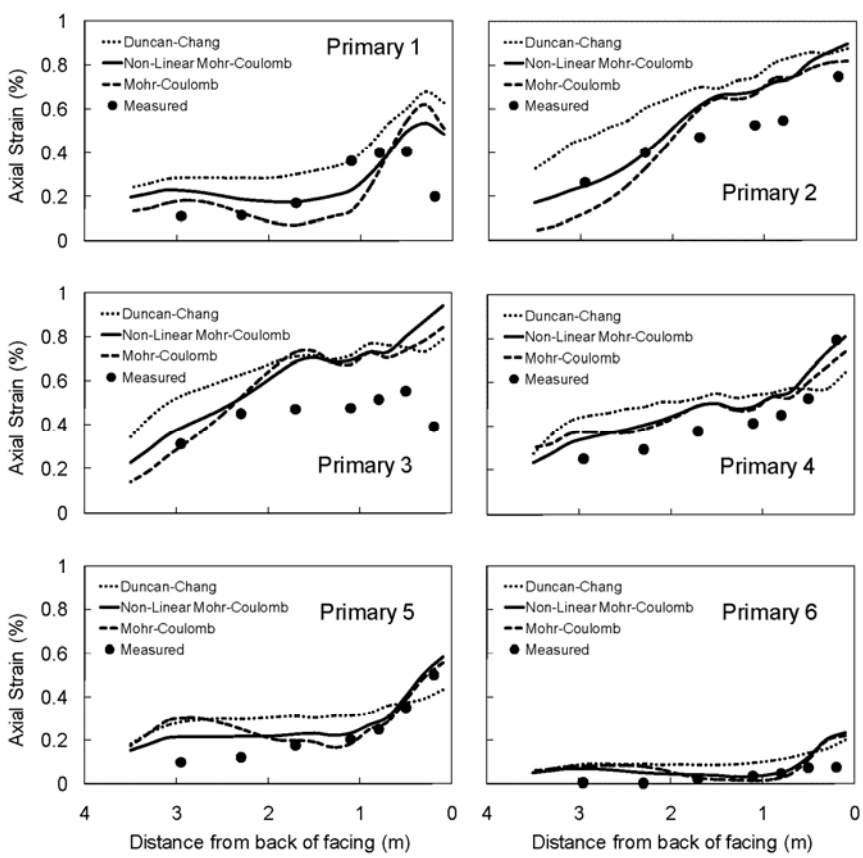

Fig. 7. Tensile strain distribution along the primary reinforcements at the end of construction height H = 6m

5. DISCUSSION

In studying the behavior of reinforced soil wall, the lateral facing displacement would be the most remarkable quantity, because it contributes directly to the wall performance and it influences other engaging factors such as reinforcement loads, as well. In the previous section, it has been shown that considering different soil constitutive models results in different prediction of wall facing deformation.

In the numerical analyses performed in this study, all elements have been considered the same, except for the soil constitutive model. The first issue that seems to be effective in the deformation pattern of the reinforced soil wall is the soil stiffness. The distribution of the calculated shear modulus in the backfill soil using different soil models are depicted in Fig. 8. Remember that the Mohr-Coulomb model considers a constant value, while the soil modulus can be varied based on the soil stress state when using the other two models. According to Figs. 8b and c, the distribution of shear modulus in the latter cases is totally different, which arises from the differences between Eqs. (1) and (3). The formulation of the Duncan-Chang model considers only the variation of the minor principal stress, while the mean principal stress is regarded as the variable in the prediction of the shear modulus of the nonlinear Mohr-Coulomb model. As a consequence, both the distribution and the value of the soil stiffness have tremendous differences between these two models. It can be concluded that a good prediction of the wall face deformation is partly dependant on a correct distribution of the shear modulus throughout the backfill soil.

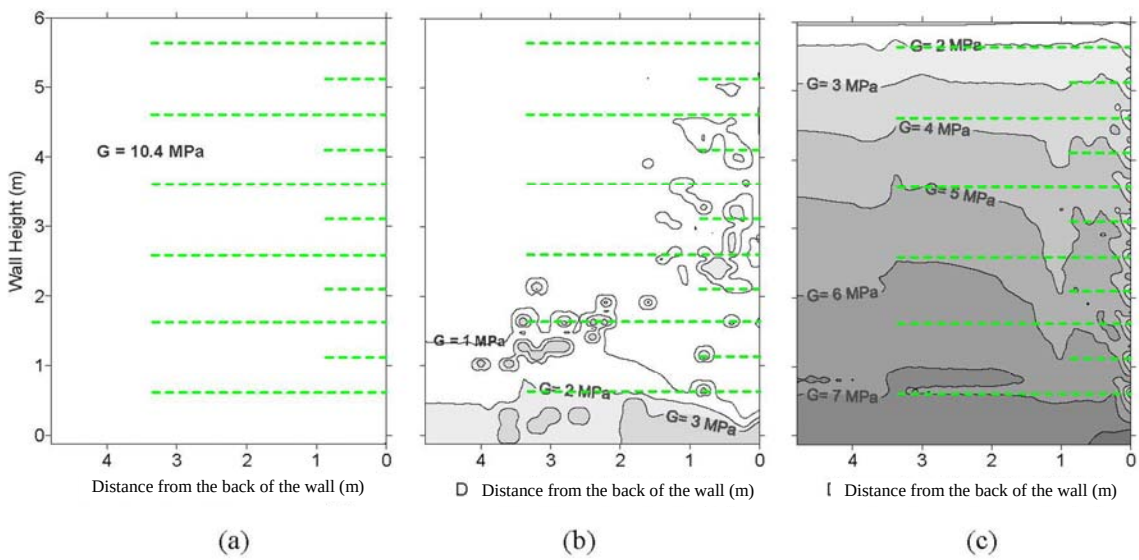

Fig. 8. Distribution of shear modulus captured by different soil constitutive models through the backfill soil: (a) Mohr-Columb; (b) Duncan-Chang; (c) Non-linear Mohr-Coulomb model

It is interesting to note that the soil stiffness by the Mohr-Coulomb model (G = 10.4 MPa) has been adopted more than twice that by the Duncan-Chang model (G < 4 MPa) and even smaller than that by the nonlinear model (G < 8 MPa), which all were derived from back fitting of single element testing (Fig. 1). However, the prediction of the wall facing displacement does not have the same order of disagreement (with about 10~20% error) as that of the stiffness modulus (with more than 200% difference). This observation is consistent with Abdelouhab et al. [29] and Ling and Leshchinsky [22], who concluded that the wall deformation is not highly sensitive to the value of the soil stiffness.

It is to be noted that stiffness (e.g., shear) moduli only describe the elastic part of the soil behavior, while dilatancy parameters take the role of the deformation in the plastic part of the behavior. In order to investigate the effect of plastic deformation behavior of the soil on the facing displacement, a hypothetical soil is simulated by the nonlinear Mohr-Coulomb model with the same set of parameters as the real soil,

but the parameter D_0 is put to zero ($D_0 = 0$) to define a contractive response (like loose soil) instead of having a dilative behavior (like dense soil). The simulated behaviors of both dilative and contractive soil single elements are plotted for comparison in Fig. 9a. The facing horizontal displacements of the walls by contractive and dilative soil behaviors are also shown in Fig. 9b. It is evident that the wall facing (horizontal displacements) with contractive soil is estimated much higher than that with the dilative soil. Such examination gives the same result as the work by Karpurapu and Bathurst [24], who showed that a correct choice of dilatancy parameters in a soil constitutive model is a necessity in accurately predicting the wall deformation.

In order to additionally investigate the effect of soil dilatancy on the wall deformation in the comparative study cited above, the distribution of the mobilized friction angle throughout the backfill is sketched in Fig. 10. According to Eq. (4), the mobilized friction angle is representative of stress state in the soil. In the case of dilative soil, the zones at the back of the blocks and narrow zones around the reinforcements (dash lines) have reached the ultimate strength ($\varphi_{mob} = 38° \sim 39°$), while in the case of contractive (loose) soil, the zones of highly mobilized shear strength are more scattered and enlarged, especially around the middle of the wall height. Referring back to Fig. 9a, it is interesting to note that the growth of deviatoric stress (or shear strength) versus axial strain in both samples is almost coincident, although the only difference in the behavior corresponds to the soil dilation. It can thus be concluded that the proposed model can easily take into consideration the effect of soil dilation, in such a way that the dilatancy controls how the shear strength mobilizes. Such investigation in the soil parameters highlights that in addition to the nonlinearity in stress-strain relationship, considering a reasonable relationship between shear strength and dilatancy parameters is essential in the soil constitutive model when using it in the analysis of reinforced soil wall response.

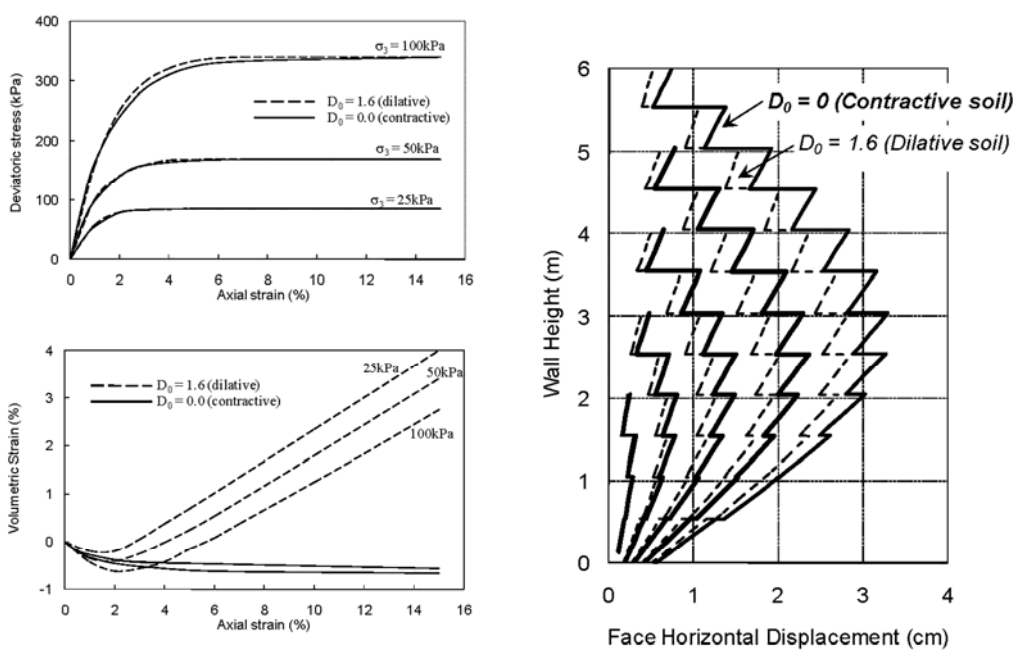

(a) (b)

Fig. 9. A parametric study on the effect of dilative/contractive behavior of the backfill soil on the deformation pattern of wall facing: (a) Comparison of dilative and contractive soil behavior simulated by the non-linear Mohr-Coulomb model; (b) horizontal displacement of wall facing simulated by dilative and contractive soil models

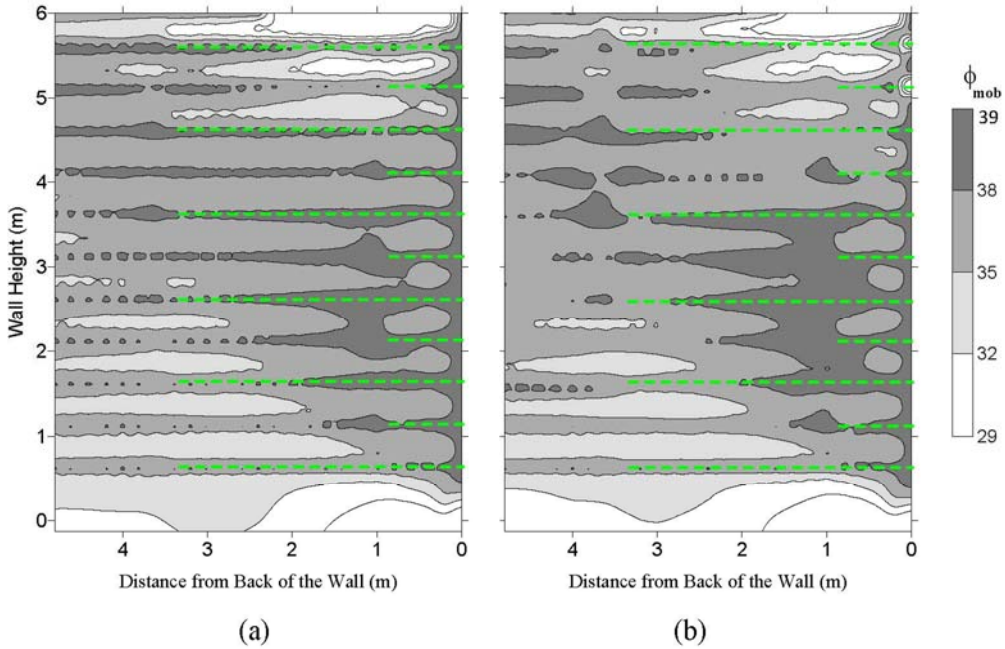

Fig. 10. Distribution of mobilized friction angle throughout the backfill soil in the case of: (a) dilative soil; (b) contractive soil. Dashed lines represents the reinforcment layers

6. CONCLUSION

In the present study, three different constitutive soil models were examined in the numerical modeling of a full-scaled reinforced soil wall. These models in the order of complexity are: linear elastic-plastic Mohr-Coulomb, nonlinear elastic Duncan-Chang, and nonlinear elastic-plastic Mohr-Coulomb models. The advantage of the second to the first one is to consider the nonlinearity in the stress-strain relationship, but its shortcoming is the inability to take into account the dilatancy. Instead, the nonlinearity in both the stress-strain relationship and the dilatancy can be captured by the third soil model proposed here. The presented model is comprised of seven parameters that can be easily obtained from laboratorial testing. The model can be considered as a developed version of the traditional Mohr-Coulomb model, whose deformation parameters are defined to be stress-dependent.

Comparison of the results obtained from the numerical analyses of the wall and the measurements reveals that:

- All these models could suitably predict the global pattern of the wall facing deformation. The difference exists in the degree of coincidence. The proposed model which simulated the soil behavior more accurately in both stress and strain spaces, gave the best accordance with the measured data.
- For an accurate prediction of the wall face displacement, it is necessary to pay attention to both elastic and plastic deformation parameters of the soil constitutive model.
- For nonlinear soil models, more agreeable result for the wall face deformation will be achievable if a reasonable distribution of the elastic stiffness is considered within the soil. The prediction accuracy is not highly sensitive to the value of the parameter, though.
- Dilatancy parameters can significantly influence the deformation of the wall. By considering a contractive behavior for the soil instead of being dilative, the facing displacement of the wall is over predicted. In addition, there should be a reasonable relationship between shear strength and dilatancy parameters.

- Using either simple or advanced soil constitutive models does not influence the prediction of the lateral stress at the back of the wall and the vertical stress over the foundation.
- The strain distribution along the reinforcement layers were correctly captured by all three soil models. Because of exclusion of the soil dilatancy in the formulation of the Duncan-Chang model, the model slightly overestimates the value of reinforcement strains with respect to the other models.

The proposed nonlinear soil constitutive model can desirably predict the static response of reinforced soil walls under monotonic loading before reaching failure or large deformations. In the current form, the formulation of the model is easy to implement in finite-element- or finite-difference-based codes. Due to the powerful bounding surface plasticity framework, the proposed model can be upgraded to simulate higher orders of the complicated soil behavior, such as cyclic loading, which requires that extra parameters be defined.

Acknowledgement: Financial support for the work reported here was provided by the Research Deputy of Ferdowsi University of Mashhad via the grant no. 22458-20/04/91.

REFERENCES

1. Liu, H., Wang, X. & Song, E. (2011). Reinforcement load and deformation mode of geosynthetic-reinforced soil walls subject to seismic loading during service life. *Geotextiles and Geomembranes*, Vol. 29, No. 1, pp. 1-16.
2. Liu, H. (2012). Long-term lateral displacement of geosynthetic-reinforced soil segmental retaining walls. *Geotextiles and Geomembranes*, Vol. 32, 0, pp. 18-27.
3. Won, M. S., Kim, Y. S. (2007). Internal deformation behavior of geosynthetic-reinforced soil walls. *Geotextiles and Geomembranes*, Vol. 25, No. 1, pp. 10-22.
4. Bathurst, R. J., Allen, T. M. & Walters, D. L. (2005). Reinforcement loads in geosynthetic walls and the case for a new working stress design method. *Geotextiles and Geomembranes*, Vol. 23, , No. 4, pp. 287-322.
5. Rowe, R. K. & Ho, S. K. (1998). Horizontal deformation in reinforced soil walls. *Canadian Geotechnical Journal*, Vol. 35, pp. 312-327
6. Totonchi, A., Askari, F. & Faerzaneh, O. (2012). Analytical solution of seismic active lateral force in retaining walls using stress fields. *Iranian Journal of Science & Technology, Transactions of Civil Engineering*, Vol. 36, No. C2, pp. 195-207.
7. Keshavarz, A., Jahanandish, M. & Ghahramani, A. (2011). Seismic bearing capacity analysis of reinforced soils by the method of stress characteristics. *Iranian Journal of Science & Technology, Transactions of Civil Engineering*, Vol. 35, No. C2, pp. 185-197.
8. Binesh, S. M. & Ghahramani, A. (2007). Elastic analysis of reinforced soils using point interpolation method. *Iranian Journal of Science & Technology, Transactions of Civil Engineering*, Vol. 31, No. B5, pp. 577-581.
9. Allen, T. M., Bathurst, R. J., Holtz, R. D., Walters, D. L. & Lee, W. F. (2003). A newworking stress method for prediction of reinforcement laods in geosynthetic walls. *Canadian Geotechnical Journal*, Vol. 40, No.5, pp. 976-994.
10. Miyata, Y. & Bathurst, R. J. (2007). Development of K-stiffness method for geosynthetic reinforced soil retaining walls construted with c-ϕ soils. *Canadian Geotechnical Journal*, Vol. 44, no. 12, pp. 1391-1416.
11. Koerner, R. M. & Soong, T. Y. (2001). Geosynthetic reinforced segmental retaining walls. *Geotextiles and Geomembranes*, Vol. 19, No. 6, pp. 359-386.
12. Helwany, S. M. B., Reardon, G. & Wu, J. T. H. (1999). Effects of backfill on the performance of GRS retaining walls. *Geotextiles and Geomembranes*, Vol. 17, No. 1, pp. 1-16.

13. Ho, S. K. & Rowe, R. K. (1994). Predicted behavior of two centrifugal model soil walls. *Journal of Geotechnical Engineering*, Vol. 120, No. 10, pp. 1845-1873.
14. Ho, S. K. & Rowe, R. K. (1996). Effect of wall geometry on the behavior of reinforced soil walls. *Geotextiles and Geomembranes*, Vol. 14, No. 10, pp. 521-541.
15. Rowe, R. K. & Ho, S. K. (1997). Continuous panel reinforced soil walls. *Journal of Geotechnical and Geoenvironmental engineering*, Vol. 123, No. 10, pp. 912-920
16. Guler, E., Hamderi, M. & Demirkan, M. M. (2007). Numerical analysis of reinforced soil retaining wall structures with cohesive and granular backfills. *Geosynthetics International*, Vol. 14, No. 6, pp. 330-345.
17. Hatami, K. & Bathurst, R. J. (2005). Development and verification of a numerical model for tha analysis of geosynthetic reinforced soil segmental walls working stress conditions. *Canadian Geotechnical Journal*, Vol. 42, No. 4, pp. 1066-1085.
18. Hatami, K. & Bathurst, R. J. (2006) A numerical model for reinforced soil segmental walls under surcharge loading. *Journal of Geotechnical and Geoenvironmental engineering*, Vol. 132, No. 6, pp. 673-684.
19. Ling, H. I., Cardany, C. P., Sun, L. X. & Hashimoto, H. (2000). Finite element study of a geosynthetic-reinforced soil retaining wall with concrete-block facing. *Geosynthetics International*, Vol. 7, No. 3, pp. 163-188.
20. Yoo, C. & Kim, S. B. (2008). Performance of a two-tier geosynthetic reinforced segmental retaining wall under a surcharge load: full-scale test and 3D finite element analysis. *Geotextiles and Geomembranes*, Vol. 26, No. 6, pp. 460-472.
21. Huang, B., Bathurst, R. J. & Hatami, K. (2009). Numerical study of reinforced soil segmental walls using three different constitutive models. *Journal of Geotechnical and Geoenvironmental engineering*, Vol. 135, No. 10, pp. 1486-1498.
22. Ling, H. I. & Leshchinsky, D. (2003). Finite element parametric study of the behavior of segmental block reinforced-soil retaining walls. *Geosynthetics International*, Vol. 10, No. 3, pp. 77-94.
23. Holtz, R. D. & Lee, W. F. (2002). Internal stability analysis of geosynthetic reinforced retaining walls. Technical report. *Washington State Transportation Commission*, Washington, D.C.
24. Karpurapu, R. & Bathurst, R. J. (1995). Behavior of geosynthetic reinforced soil retaining walls using the finite element method. *Computers and Geotechnics*, Vol. 17, pp. 279-299.
25. Desai, C. S. & El-Hoseiny, K. H. (2005) Prediction of field behavior of reinforced soil wall using advance constitutive model. *Journal of Geotechnical and Geoenvironmental engineering*, Vol. 131, No. 6, pp. 729-739.
26. Ling, H. I., Liu, H., Kaliakin, V. N. & Leshchinsky, D. (2004). Analyzing dynamic behavior of geosynthetic-reinforced soil retaining walls. *Journal of Engineering Mechanics*, Vol. 130, No. 8, pp. 911-920.
27. Ling, H. I. & Liu, H. (2009). Deformation analysis of reinforced soil retaining walls- simplistic versus sophisticated finite element analyses. *Acta Geotechnica*, Vol. 4, doi:10.1007/s11440-009-0091-6, pp. 203-213.
28. Lade, P. V. (2005). Overview of constitutive models for soils. In: Yamamuro JA, Kaliakin VN (eds) Soil Constitutive models: Evaluation, selection, and calibration. *ASCE Geotechnical special publication, Geo-Frontiers Conference.*
29. Abdelouhab, A., Dias, D. & Freitag, N. (2011). Numerical analysis of the behaviour of mechanically stabilized earth walls reinforced with different types of strips. *Geotextiles and Geomembranes*, Vol. 29, No. 2, pp. 116-129.
30. Seyedi Hosseininia, E. & Farzaneh, O. (2010). Development and validation of a two-phase model for reinforced soil by considering nonlinear behavior of matrix. *Journal of Engineering Mechanics*, Vol. 136, No. 6, pp. 721-735.
31. Seyedi Hosseininia, E. & Farzaneh, O. (2009). A simplified two-phase macroscopic model for reinforced soils. *Geotextiles and Geomembranes*, Vol. 28, pp. 85-92.

32. Lade, P. V. & Duncan, J. M. (1973). Cubical triaxial tests on cohesionless soil. *Journal of Soil Mechanics and Foundations Division, ASCE*, Vol. 99, SM10, pp. 793-812.
33. Zienkiewicz, O. C., Humpheson, C. & Lewis, R. W. (1975). Associated and nonassociated visco-plasticity and plasticity in soil mechanics. *Géotechnique*, Vol. 25, No. 4, pp. 671-689.
34. Vermeer, P. A. & de Borst, R. (1984). Non-associated plasticity for soils, concrete and rock. *Heron*, Vol. 29, No. 3, pp. 1-64.
35. Duncan, J. M., Byrne, P., Wong, K. S. & Mabry, P. (1980). *Strength, stress-strain and bulk modulus parameters for finite element analysis of stress and movements in soil masses*. University of Berkeley, California
36. Duncan, J. M. & Chang, C. Y. (1970). Nonlinear analysis of stress and strain in soils. *Journal of Soil Mechanics and Foundations Division, ASCE*, Vol. 99, SM5, pp. 1629-1653.
37. Dafalias, Y. F. & Popov, E. P. (1975). A model of nonlilearly hardening materials for complex loading. *Acta Mechanica*, Vol. 21, pp. 173-192.
38. Krieg, R. D. (1975). A practical two-surface plasticity theory. *Journal of applied Mechanics, ASME*, Vol. 42, pp. 641-646.
39. Li, X. S. (2002). A sand model with state-dependent dilatancy. *Géotechnique*, Vol. 52, No. 3, pp. 173-186.
40. Yang, B. L., Dafalias, Y. F. & HeRrmann, L. R. (1985). A bounding surface plasticity model for concrete. *Journal of Engineering Mechanics*, Vol. 111, No. 3, pp. 359-380.
41. Dafalias, Y. F. (1986). Bounding surface plasticity, I: Mathematical foundation and hypoplasticity. *Journal of Engineering Mechanics*, Vol. 112, No. 12, pp. 1263-1291.
42. Tajiri, N., Sasaki, H., Nishimura, J., Ochiai, Y. & Dobashi, K. (1996). Full-scale failure experiments of geotextile-reinforced soil walls with different facings. *IS-Kyushu 9, third International symposium on earth reinforcement*, Balkema, Rotterdam, the Netherlands.
43. Al Hattamleh, O. & Muhunthan, B. (2005). Numerical procedures for deformation calculations in the reinforced soil walls. *Geotextiles and Geomembranes*,Vol. 24, No. 1, pp. 52-57.
44. Itasca Consulting Group (2000). *FLAC: Fast Lagrangian Analysis of Continua*. 4.0 edn. Itasca Consulting Group, Minneapolis.